

Digitized Heat Transfer: A New Paradigm for Thermal Management of Compact Micro Systems

Eric Baird and Kamran Mohseni, *Member, IEEE*

Abstract—This paper presents theoretical and numerical results describing digitized heat transfer (DHT), a newly developing active thermal management technique for high-power density electronics and integrated micro systems. In describing DHT, we numerically investigate the mass, momentum, and energy equations governing the flow within a translating microdroplet. Our analysis shows the existence of a pair of recirculation zones inside the droplet. This internal circulation within discrete fluid slugs results in significantly increased overall heat transfer coefficients when compared to continuous Graetz-type flows. The internal circulation drives the cold fluid in the middle of the droplet to the vicinity of the walls and creates a higher local temperature difference between the wall and the fluid in contact with the wall, resulting in higher heat transfer rates. Nusselt numbers characterizing DHT flow are also shown to exhibit periodic fluctuations with a period equal to the characteristic time scale for droplet circulation. The overall effect of discretizing a flow on heat transfer capability is described and characterized in terms of a nondimensional circulation number defined by the ratio of characteristic thermal diffusion and fluid circulation time scales. DHT coolants, including liquid metals and alloys, are proposed, and their physical properties are shown to enable handling of significantly higher heat transfer rates than classical air- or water-cooled methods. The actuation method for DHT coolant transport is also outlined, and shown to provide the capability for active, on-demand suppression of transient hot spots. This overall analysis defines the key parameters for optimization of the DHT method and forms the basis of ongoing experimental work.

Index Terms—Convective heat transfer, digitized heat transfer (DHT), electrowetting, Graetz problem, thermal management.

I. INTRODUCTION

INCREASED heat rejection requirements are one of the primary limiting factors in developing the next generation of compact electronics [1]; examples include such common items as laptop computers, palm pilots, lasers and micro-scale avionics. The conversion of electrical energy to thermal energy is an unavoidable byproduct of the normal operation of any electronic device. If not properly managed, the resultant increase in substrate temperature can reduce functioning efficiency, or even cause complete system failure. In addition, excess heat can increase signal noise in a semiconductor by increasing the movement of free electrons.

Manuscript received January 25, 2006; revised July 12, 2007. This work was supported by the National Science Foundation under an exploratory research grant and NSF Contract CTS-0540004 and by DARPA under Contract W911NF-07-1-0186. This work was recommended for publication by Associate Editor K. Ramakrishna upon evaluation of the reviewers' comments.

The authors are with the Department of Aerospace Engineering Sciences, University of Colorado, Boulder, CO 80309-429 USA (e-mail: kamran.mohseni@colorado.edu).

Color versions of one or more of the figures in this paper are available online at <http://ieeexplore.ieee.org>.

Digital Object Identifier 10.1109/TCAPT.2008.916810

Furthermore, a reduction in circuit delay (and therefore an increase in speed) is often achieved by increasing circuit packaging densities while simultaneously raising the power dissipation per circuit. As a result of this ever-growing demand for smaller, more powerful compact electronic devices, heat flux rejection requirements are increasing at a challenging pace; heat generation rates in excess of 250 W/cm^2 have already been predicted for some emerging technologies [2], [3]. The development of efficient micro scale thermal management methods for handling such high flux densities is a primary roadblock in developing the next generation of compact microdevices [1].

Traditionally, heat has been removed from an electronic system to the surrounding environment through air-cooled heat sinks. A significant decrease in thermal resistance and orders of magnitude increase in heat removal, however, can be achieved by using liquid cooling instead of air. The potential for direct integration of liquid-carrying microchannels inside a heat-generating substrate is particularly attractive, as thermal contact resistance could be avoided. The concept of liquid cooling through microchannels was first explored more than two decades ago by Tuckerman and Pease [4]. A comprehensive review of microchannel transport is found in [5], while cooling of high-power microdevices using liquid metals is explored in [6]. Other methods of micro scale thermal management currently under research include microjet devices proposed in [7] and thermionic cooling described in [8], [9], as well as thermoelectric microcoolers such as the one explored in [10].

In addition to steady state cooling requirements, concentrated areas of high heat flux (two to three times more than the average chip flux) also emerge during the operation of an electronic device such as an integrated chip (IC). These areas, often referred to as “hot spots,” require special techniques for thermal management. Ideally, transient local heat spikes should be targeted individually and on-demand to most efficiently maintain the substrate below a predefined maximum temperature, a degree of control unavailable from classical heat transfer methods such as air fans or continuous liquid flows. Rather than continuous flows, these areas can be specifically and efficiently targeted through the use of individual droplets.

The use of discrete droplets for small-scale applications is an emerging field known as “digital microfluidics,” and has a wide range of possible applications [11]–[21]. In an analogous way, here, we refer to the use of an array of discrete microdroplets for thermal management as “digitized heat transfer” (DHT) [22]. DHT using liquid alloy electrowetting has been proposed by Mohseni [22]–[25]. The main advantage of using liquid alloy droplets over other liquids such as water or oil [26] is the much higher thermal conductivity of alloys, making it ideal for heat removal. In DHT, a series of microdroplets can be used for continuously cooling a substrate, or specific hot spots may be in-

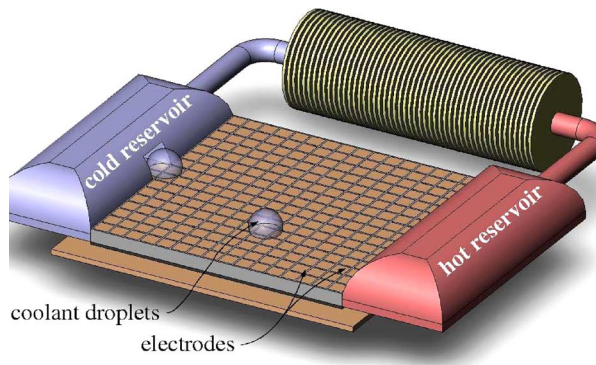


Fig. 1. Schematic of a DHT device. The droplets are sitting on the hot substrate patterned with electrodes and dielectric coating. Note that the patterned electrodes could be equally located on a covering plate on top of the device instead of the hot plate. There is no need for side walls.

dividually targeted as they arise. In each case, the fluid absorbs thermal energy through conduction at its contact with the substrate and removes the energy to an external heat sink via bulk motion of the droplet. Droplets are dispensed from a cold pool, transported over the heated area and through an external heat sink, then returned to the fluid reservoir. Each of these steps is accomplished solely through the application of a voltage to an individually addressable array of electrodes patterned directly onto the heated surface; as a consequence, DHT may be carried out for droplets between top and bottom plates with or without channel sidewalls. The system has no moving parts whatsoever to wear out or break, and the power requirement for fluid transport is extremely low. Unlike continuous flows, digitized microfluidic systems do not suffer from the very high pressure head normally encountered in microchannels [2], [5]. The digitization method facilitates the use of a hierarchical and cell-based approach for microfluidic system design. In this case, the fluid handling can be treated in a discrete manner and based on basic programming instructions for droplet transport, mixing, storage, cutting, and merging. A complex microfluidic operation can be easily built by an electrode activation program to launch a sequence of basic instructions, as seen in Fig. 1.

In traditional thermal management, heat is continuously transported by both conduction and convection throughout a continuous flow. As demonstrated in Fig. 1, with DHT thermal energy is instead transported in discrete bundles within individual droplets. These droplets may be continually dispensed in a closely spaced array for steady state cooling, or individually used to target transient hot spots. This provides a much greater degree of flexibility and control when compared to continuous flows in rigid channels. Each droplet is essentially independent of all the others, or at most weakly correlated by the ambient air. This is a fundamental disparity between continuous and digitized flows, and its effect must be addressed when solving for physical characteristics of DHT such as the Nusselt number.

The most important hydrodynamic differences between DHT droplets and classical thermal entry flow in a heated channel are the introduction of internal circulation within the fluid slugs and the limiting of axial convection and diffusion as shown in [24]. Internal mixing, caused by the flow's radial velocity near the impermeable front and rear faces of each droplet, significantly increases fluid heating in the high Peclet number regime; that

is, when the convection time scale is less than the diffusion time scale. As a consequence, not only does DHT provide marked improvements over continuous flows in terms of fabrication, actuation, and control, but also enhanced heat transfer coefficients when the digitized flow is carefully optimized and handled.

Effective methods of actuating discrete droplets at very small scales must also be explored. In micro scale, surface tension forces, which scale linearly with the characteristic length, dominate forces proportional to higher powers of the length scale, such as pressure and body forces. Because of fast response times, low power consumption and low heat generation, electrostatic methods show the most promise for use in DHT [12], [13], [27], [28]. Electrowetting on dielectric (EWOD), in which an electrostatic force localized near the tri-phase contact line is generated by the application of an electric field transverse to the direction of flow, has the same scaling as surface tension and is a relatively simple method to both fabricate and control [29], [30]. EWOD has already been shown to be a reliable, efficient technique for transporting discrete droplets of electrically conductive aqueous solutions [12], [19], [31]. In DHT, EWOD will be used to dispense and transport thermally conductive liquid slugs for both steady state cooling and on-demand suppression of transient heat spikes. Other methods, such as continuous electrowetting (CEW), dielectrophoresis (DEP) and thermocapillary pumping (TCP), may also be viable alternatives for certain devices [14], [22], [30], [32]–[40]. The device pictured in Fig. 1 uses EWOD as the actuating force.

Digitized microfluidics also allows for the use of novel cooling fluids. Water is often used as a coolant instead of air because its thermal conductivity is over 20 times higher, allowing it to support much greater heat flux densities. Liquid metals and alloys, on the other hand, possess thermal conductivities another 1–2 orders of magnitude greater than water's. While their higher thermal conductivities are partially offset by lower values of specific heat, liquid metals and alloys present a significant advantage over classical coolants for quickly absorbing large amounts of thermal energy in very small regions. Several alloys which are liquid at room temperature and possess favorable thermal properties and are completely nontoxic are now commercially available. While non-aqueous liquids are not yet commonly used in digitized microfluidics, EWOD may theoretically be used to transport any electrically conducting fluid; EWOD-actuation of a $0.5 \mu\text{L}$ droplet of Galinstan liquid alloy has been observed in our lab.

The remainder of this paper is organized as follows: In Section II, a brief overview of digital microfluidics is given, including the EWOD actuation method and the flow field inside a translating microdroplet. In Section III, the novel method of DHT is proposed and described. Section IV presents analytical and numerical analyses characterizing the heat transfer properties of discretized droplets, with a brief summary of results given in Section V.

II. DIGITAL MICROFLUIDICS

Continuous flows in rigid, closed microchannels can be inefficient. Systems designed with steady flows in permanently formed channels often suffer from complex fabrication, complicated integration and control, and large amounts of wasted

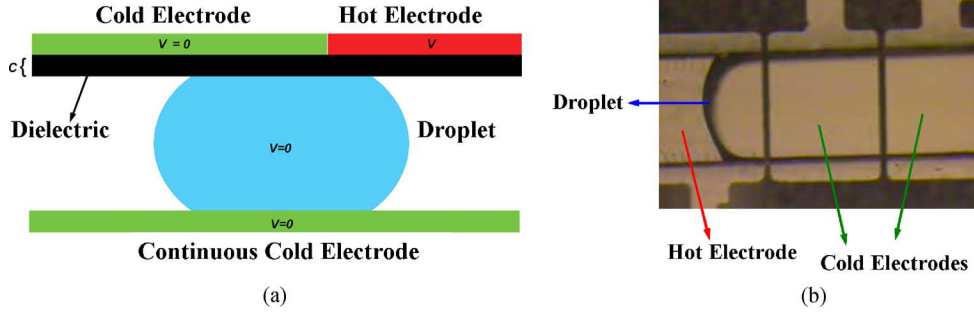


Fig. 2. (a) Side view depiction of a single EWOD-actuated microdroplet. (b) Top view photograph of an EWOD device used in the authors' laboratory. The top plate of the channel is transparent.

fluids [12]. These drawbacks may be reduced through the use of discrete droplets instead of continuous flows, as described in the introduction. When individual droplets are used, fixed volumes of liquid may be precisely manipulated on a fabricated grid of electrodes via electrowetting on dielectric; this reduces actuation voltages, power consumption and the required amount of fluid while simultaneously increasing the degree of programmability and control. In this section we present a brief overview of the EWOD force and resulting fluid velocity, as well as details of the flow field inside an EWOD-actuated droplet.

A. Electrowetting on Dielectric

Droplet transport via EWOD can be carried out for sessile droplets on flat surfaces, between two flat plates or inside a micro channel or pipe. In each case, a patterned grid of electrodes is coated with a thin layer of insulation, creating a high capacitance between the electrode array and the conducting fluid, as seen in Fig. 2 [29]. For the simple configuration considered here, the droplet is grounded by the continuous cold electrode and a voltage is swept along the channel such that the fluid's front, but not rear, is always beneath a hot electrode with applied voltage V relative to ground. The channel height, H , is assumed to be much greater than the dielectric thickness. This configuration results in a constant forward force per unit width on the droplet's contact line of

$$F_x = \frac{1}{2}cV^2 \quad (1)$$

where V is the applied voltage and c is the capacitance, per unit area, of the dielectric layer. We may use this force per width to find an equivalent pressure gradient along the droplet, driving the flow. Ignoring edge effects near the front and rear interfaces, this may then be substituted into a simplified Navier–Stokes equation to find the final steady state bulk velocity of an EWOD-actuated slug

$$U = \frac{cV^2 H}{24\mu L} \quad (2)$$

where μ is the fluid's viscosity and H/L is its height-to-length ratio; see [30] for details. Note that this velocity is independent of scale, depending only on the droplet's aspect ratio. As a consequence, EWOD is able to sustain reasonable fluid velocities (up to 1 m/s) at very small scales without the need of extremely high pressure gradients. The expression given in (2) is for the average slug velocity of a droplet. In other words, it is the velocity

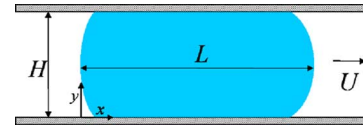


Fig. 3. Droplet in channel (side view). The droplet may be either unconstrained in the direction normal to the page or in contact with sidewalls. In this paper, we consider a droplet in a thin, rectangular microchannel, with the fluid in contact with the channel on four sides and having a free meniscus at its front and rear.

of the front and rear interfaces relative to the channel walls, and is equal to the integrated average of the axial component of the droplet's internal flow field.

B. Droplet Hydrodynamics

We again consider a microchannel of height H and width w containing a fluid droplet of length L , viscosity μ and density ρ , as seen in Fig. 3. For simplicity we assume $w \gg H$, such that the flow can be considered two-dimensional and there is no z dependence.

We apply no-slip boundary conditions along the top and bottom walls. The droplet is able to translate while simultaneously satisfying the no-slip condition through a dual rolling motion: Torques produced by viscous drag along the channel walls induce twin hollow vortices in the droplet of equal magnitude but opposite sign. As the droplet itself moves forward, internal circulation ensures that the fluid adjacent to the top and bottom walls is stationary at all times [24]. An internal circulation has also been observed in [26]. On the front and rear interfaces, we apply the free interface stress condition, given by

$$\hat{n} \cdot \vec{\tau} = 2K\sigma\hat{n} \quad (3)$$

where \hat{n} is the unit normal vector to the surface, $\vec{\tau}$ is the stress tensor in the fluid, K is the mean curvature, and σ is the surface tension. To reduce the number of free parameters in the preliminary calculations presented in this paper, we consider the product of the interface curvature and the surface tension coefficient to be very small, and apply a simpler zero stress condition on these surfaces. This is equivalent to letting the Weber number

$$\text{We} = \frac{\rho U^2 H}{\sigma} \quad (4)$$

tend to infinity. This has the effect of eliminating any vorticity produced at the front and rear interfaces, slightly reducing droplet mixing when compared to the case of more rigid caps.

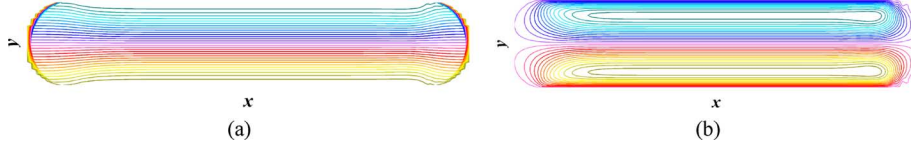


Fig. 4. Droplet streamlines in lab frame (a) and droplet frame (b). This data was obtained for a droplet with $Re = 100$ and a contact angle of 135° .

Due to the droplet geometry, it is convenient to consider the governing equations in the streamfunction-vorticity ($\psi - \omega$) formulation, such that

$$u = \frac{d\psi}{dy} \quad (5)$$

$$v = -\frac{d\psi}{dx} \quad (6)$$

$$\omega = \frac{\partial v}{\partial x} - \frac{\partial u}{\partial y}. \quad (7)$$

If we assume the effect of the surrounding atmosphere between droplets is negligible, such that each fluid slug may be considered as independent and uncoupled from all the others, a convenient frame of reference for solving for fluid flow is the frame in which an individual droplet is at rest. In this frame, the droplet's center of mass remains stationary while the side-walls move at a constant velocity of $-U$, where U is the bulk (average) axial speed of an individual droplet. Each droplet is then essentially a modified cavity flow; following convention, we nondimensionalize the time t by H/U , the velocities by U , and the axial coordinate x , radial coordinate y and droplet length L by H . The divergence and momentum equations governing the flow inside a droplet then reduce to

$$\frac{\partial \psi}{\partial t} = \frac{\partial^2 \psi}{\partial x^2} + \frac{\partial^2 \psi}{\partial y^2} + \omega, \quad (8)$$

$$\frac{\partial \omega}{\partial t} = \frac{1}{Re} \frac{\partial^2 \omega}{\partial x^2} + \frac{1}{Re} \frac{\partial^2 \omega}{\partial y^2} - u \frac{\partial \omega}{\partial x} - v \frac{\partial \omega}{\partial y}. \quad (9)$$

(10)

Here, $Re = \rho U H / \mu$ is the Reynolds number. We take ψ to be 0 on all the boundaries and the condition on ω is calculated via Thom's formula [41] at the top and bottom solid walls. As a result of the zero stress condition, $\omega = 0$ on the free interfaces. When solving for the heat transfer into a DHT droplet, we will assume that the flow is already hydrodynamically fully developed before entering the heated region; the flow field is calculated via successive over-relaxation with a relatively strict convergence criterion before applying the heated boundary condition. Contour plots of the droplet streamfunction in both the lab frame and the rest frame of the droplet are found in Fig. 4.

In the lab frame, away from the front and rear faces the droplet has the standard parabolic profile characteristic of Poiseuille flow. The velocity of each point in the droplet is non-negative, and the streamlines do not form closed paths in space. In the rest frame of the droplet, however, the velocity profile is given by subtracting the droplet's average speed

$$u(y) = 6U \left(\frac{y}{H} - \frac{y^2}{H^2} - \frac{1}{6} \right). \quad (11)$$

In this reference frame, the droplet is symmetrically split into twin hollow vortices centered at the roots of the velocity pro-

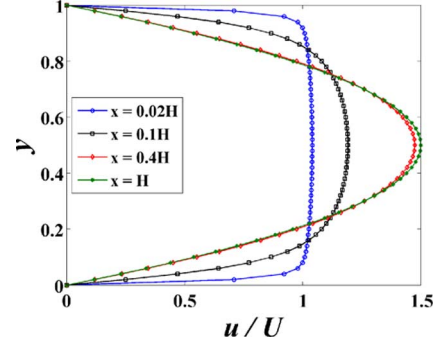


Fig. 5. Velocity profiles at several locations in a translating microdroplet with straight sides and $L = 2H$. y has been nondimensionalized by H , u is the local velocity, and U is the bulk velocity of the droplet. Distances are measured forward from the trailing edge.

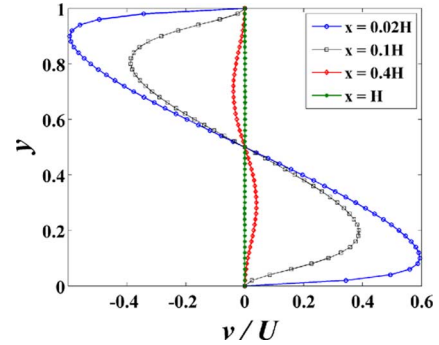


Fig. 6. Radial velocities at several different cross-sections in a translating microdroplet and $L = 2H$. y has been nondimensionalized by H , v is the local radial velocity, and U is the bulk (axial) velocity of the droplet. Note that the radial velocity is significant near the droplet interfaces, but disappears towards the center. This radial convection, which is not present in continuous channel flows, increases droplet mixing and enhances heat transfer into the fluid.

file, $y = (1/2 \pm \sqrt{12}/12)H$. When edge effects are included, the streamlines form closed paths within the droplet. These vortices result in an internal mixing, carrying heat away from the walls towards the droplet's center. Fig. 5 presents the axial velocity profile for several axial locations inside a droplet. Note that near the interfaces, the profile flattens into that of uniform slug flow at the bulk velocity, whereas away from the walls the profile approaches the perfect parabola characteristic of Poiseuille flow.

Fig. 6 gives a plot of v , the radial velocity component, as a function of y at the same cross-sections within the droplet. This radial convection brings unheated fluid to the walls at the droplet's front and carries heated fluid from the exterior to the droplet's center at the rear. This internal circulation is not present in continuous channel flows, and serves to increase heating within a fluid slug.

The importance of the recirculation effect in determining the Nusselt number is governed by a dimensionless parameter we refer to as the "circulation number." From dimensional analysis

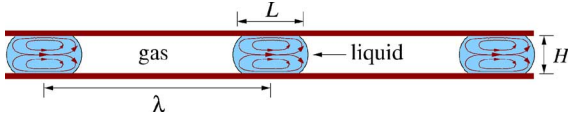
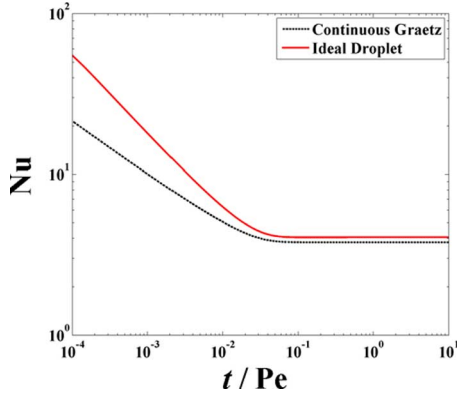


Fig. 7. Evenly spaced liquid droplets in a microchannel.

Fig. 8. Nusselt number plots in thermal entry region of a parallel plate microchannel for a continuous flow and an idealized (zero internal convection) discretized droplet. The two solutions differ by less than 10% in the asymptotic limit, but the effect of axial convection results in significantly different results for small values of t/Pe [24].

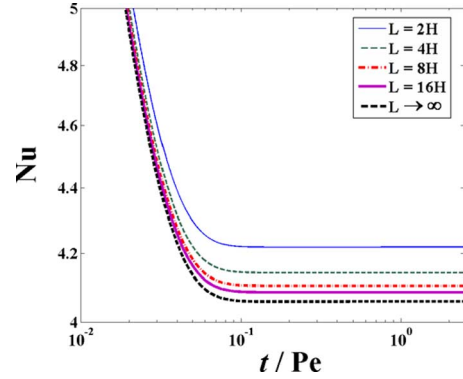
of the governing equations, the characteristic time for thermal diffusion into the droplet is given by $\tau_{\text{diff}} = H^2/\alpha$. The characteristic time for one full internal recirculation is simply $\tau_{\text{circ}} = (H + 2L)/U$. The ratio of these determines the relative effect of the internal convection:

$$N_{\Gamma} = \frac{\tau_{\text{diff}}}{\tau_{\text{circ}}} = \frac{UH^2}{\alpha(H + 2L)} = \text{Pe} \frac{H}{H + 2L} \quad (12)$$

where $\text{Pe} = UH/\alpha$ is the Peclet number and all other variables are as defined previously. $H + 2L$ is seen to be the distance traveled by a droplet when making a single complete internal revolution. For values of N_{Γ} greater than unity, circulation will significantly increase heat transfer; a fluctuation in Nusselt number with a period given by τ_{circ} will be clearly demonstrated in Fig. 10 of Section IV. The magnitude of the oscillation is continuously dampened as the droplet advances and nears the wall temperature. For digitized flows with small values of N_{Γ} , such as very slowly moving droplets or fluids with extremely high thermal diffusivities, circulation will have very little effect on Nusselt Number.

III. DIGITIZED HEAT TRANSFER

A high-performing electronic device requires a large heat flux to maintain its optimal operation, and transient surface hot spots may cause rapid system failure. To remedy this situation, we propose the use of discrete droplets for on-demand thermal management in continuous response to system requirements. A schematic of our heat management device was given in Fig. 1. The EWOD actuation method, described in Section II, will be used to transport liquids from a dispensing pool to hot spots on a chip. The EWOD pumping process is especially promising, as it transports electrically conductive fluids (such as liquid alloys or aqueous solutions), requires very little power, does not generate heat itself and uses relatively low voltages [42].

Fig. 9. Log-log plot of Nusselt numbers for droplets of liquid metal for various values of L/H . Here, the Peclet number is low ($\text{Pe} = 0.35$), and the effect of internal convection is small; the difference between solutions for various values of L/H is therefore minimal. Note the small scale on the y -axis.

As mentioned in the introduction, the concept of liquid cooling through microchannels was explored more than two decades ago by Tuckerman and Pease [4]. They chemically etched a $50 \mu\text{m} \times 300 \mu\text{m}$ microchannel in a $1 \text{ cm} \times 1 \text{ cm}$ silicon chip and removed heat at a rate of 790 W by pumping water through the channel. At this heat rejection rate they observed a 71°C temperature difference in the water. For a complete review of the available techniques for thermal management of electronic circuits, the reader is referred to [43]–[45] and the references therein.

Because of their high thermal conductivities, the most effective liquids for supporting heat transfer are metals and alloys [23]. Mercury, which is easily and effectively mobilized by electrowetting, is one option. Lee and Kim [39] demonstrated the continuous electrowetting transport of mercury droplets in sulfuric acid at 4 cm/s using a 1–3 V driving voltage. The power consumption was 10–30 μW at an average current of only 10 μA .

Mercury is toxic, however, and is not recommended for general use in cooling systems. On the other hand, liquid alloys have the same advantages as mercury, but the metals in these alloys are nontoxic. In addition, the vapor pressures of these liquids are substantially lower than mercury's. A variety of Gallium/Indium/Tin alloys which are liquid at room temperature are now easily available. The most important aspect of these alloys for their application in DHT is their high thermal conductivities, which can be several times greater than mercury's. These characteristics suggest that liquid alloy electrowetting can achieve heat flux removal capabilities far beyond many other alternative techniques. Physical properties of some liquid metals and alloys are listed in Table I (table taken from [23]).

In DHT, the system has no moving mechanical parts to leak, wear out, or stick. Therefore, no lubricants are required. By using discrete droplets, any need for valves and pumps is eliminated and all the basic fluidic operations can be achieved by correctly applying a voltage to the system. The current technique can be used for active thermal management of integrated circuits and compact microsystems to detect and properly handle an over-heating event. This is in contrast to passive heat dissipation mechanisms, such as heat sinks and fans, that require continuous coolant flow.

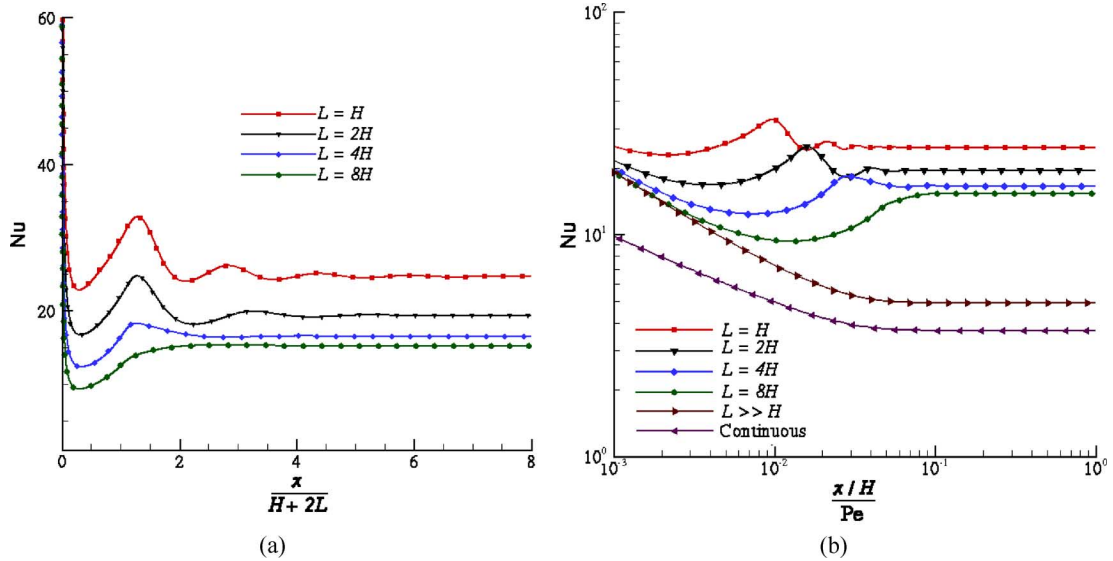


Fig. 10. (a) Nusselt numbers in the entry region of a thermally developing flow, normalized by the length of one circulation within the droplet. $Re= 100$ and $Pe= 500$ for each curve. Note that the frequency of the oscillations in each curve is roughly equal to the frequency of circulation within the droplet, and that the effect is damped out more quickly for longer droplets. (b) Log-log plot of Nusselt numbers versus $(x/H)/Pe$, the usual variable used in plotting results from the Graetz problem [41].

TABLE I
PHYSICAL PROPERTIES OF SOME LIQUID METALS AND ALLOYS.

Liquid metal or alloy	Density ρ kg/m ³	Melting point °C	Boiling point °C	Thermal cond. k W/mK	Specific heat C J/kg/°C	viscosity μ kg/ms = N s/m ²	surface tension σ N/m
Water	1000	0	100	0.6	4184	0.86×10^{-3}	0.0717
Mercury	13546	-39	356	8.4	140	0.15×10^{-3}	0.47
Galinstan	6440	-19	> 1300	16.5	–	2.4×10^{-3}	–
Gallium	6093	29.98	1983	33.49	343.32	1.89×10^{-3}	0.735
Indalloy 46L	6499	7.6	–	–	–	–	–
Indalloy 51	6499	10.7	–	–	–	–	–

Another advantage of digitized liquid alloy electrowetting is in the suppression capability for temperature overshoots during the dissipation of transient power spikes. In many applications, thermal transients last for only a short period. Consequently, no continuous operation is needed. In such cases digitized droplets can be mobilized, if needed, to address local thermal management demands. Furthermore, the latent heat of phase change of such alloys can be exploited for phase change thermal energy storage [46]. Since the temperature of the alloy remains more or less constant during melting, droplets of such alloys can be used for thermal management of transient power spikes.

It should be noted that one could expect to transport liquid droplets of most materials at low temperature through some method of electrostatic actuation. As a result, a potential version of DHT would use cryogenic liquids. Some of the more common cryogenic liquids include Helium-3, Helium-4, Hydrogen, Neon, Nitrogen, air, Argon, Oxygen, and Methane, which are all in liquid forms at temperatures below -201 °C.

IV. THERMAL MANAGEMENT ANALYSIS

A full solution describing DHT requires numerically solving the coupled Navier-Stokes, energy, and continuity equations.

In this section, we use the fully-developed fluid flow found in Section II-B as an input into the general thermal transport equation. To simplify the analysis in identifying the basic thermal characteristics of DHT, in this section we consider only rectangular droplets and ignore the effect of meniscus curvature on our results. The shape of the fluid meniscus and its influence on heat transfer will be included in future publications.

We consider droplets of length L whose centers of mass are separated by a distance λ in an infinitely long microchannel of height H , as in Fig. 7. The droplets enter a heated region at a uniform temperature T_{in} , and move at a constant velocity U , which for EWOD is given by (2). The distance between droplets is related to the fluid velocity by

$$\lambda = U\tau \quad (13)$$

where τ is the time between droplets entering the channel. The channel walls are held at a constant temperature T_{wall} , and the droplet temperature is denoted by T , with T_{avg} indicating the average temperature of an entire slug.

A. Scale Analysis

We consider only two dimensions, and assume the problem is symmetric in the z (into the page) direction. All heat fluxes are calculated per unit area on the channel wall; as the problem is symmetric in the z direction, the droplet width, w , does not appear.

The full, dimensional equation for the developing temperature field inside a fluid slug is given by

$$\frac{\partial \theta}{\partial t} + u \frac{\partial \theta}{\partial x} + v \frac{\partial \theta}{\partial y} = \alpha \left(\frac{\partial^2 \theta}{\partial x^2} + \frac{\partial^2 \theta}{\partial y^2} \right) \quad (14)$$

where $\alpha = k/\rho C$ is the thermal diffusivity of the fluid and

$$\theta = \frac{T - T_{\text{wall}}}{T_{\text{wall}} - T_{\text{in}}}. \quad (15)$$

k is the fluid's thermal conductivity, and C is its specific heat capacity. We scale the coordinates appropriately by letting $x^* = x/L$, $y^* = y/H$, and $t^* = t/(H/U)$. Substituting this in and dropping the stars for notational convenience, the equation then reduces to

$$\frac{U}{H} \frac{\partial \theta}{\partial t} + \frac{1}{L} u \frac{\partial \theta}{\partial x} + \frac{1}{H} v \frac{\partial \theta}{\partial y} = \alpha \left(\frac{1}{L^2} \frac{\partial^2 \theta}{\partial x^2} + \frac{1}{H^2} \frac{\partial^2 \theta}{\partial y^2} \right). \quad (16)$$

To this point, $u(x, y)$ and $v(x, y)$ are still the full, dimensional velocities, which must also be nondimensionalized. The scaling of u , the wall velocity U , is clear, so we let $u^* = u/U$. The effect of v , however, is more complex. As shown in Section II-B, the radial velocity is centralized within about H of the droplet's interfaces. For a long droplet, v will only have a reasonable magnitude in a narrow band near the droplet edges, and its influence must therefore vanish as $L/H \rightarrow \infty$. For a more narrow droplet, it will be much more important. The incompressible continuity equation is given by

$$\frac{\partial u}{\partial x} + \frac{\partial v}{\partial y} = 0 \quad (17)$$

from which we may deduce a convenient scaling for the axial velocity, V

$$\frac{U}{L} \sim \frac{V}{H} \Rightarrow V \sim \frac{HU}{L}. \quad (18)$$

Letting $v^* = v/(UH/L)$, substituting in and again dropping the star for convenience, the energy equation now reads

$$\frac{\partial \theta}{\partial t} + \frac{H}{L} u \frac{\partial \theta}{\partial x} + \frac{H}{L} v \frac{\partial \theta}{\partial y} = \frac{1}{\text{Pe}} \left(\frac{H^2}{L^2} \frac{\partial^2 \theta}{\partial x^2} + \frac{\partial^2 \theta}{\partial y^2} \right) \quad (19)$$

where $\text{Pe} = UH/\alpha$ is the Peclet number, a common dimensionless number used to compare the effects of convection and thermal diffusion in a fluid. When Pe is greater than unity, internal convection will be important to the developing temperature field. When Pe is small, radial diffusion will dominate.

In this formulation, the boundary and initial conditions on $\theta(t, x, y)$ are uniquely specified as $\theta(0, x, y) = 1$, $\theta(t, x, 0) = 0$, $\theta(t, x, 1) = 0$, $(\partial \theta / \partial x)(t, 0, y) = 0$, and $(\partial \theta / \partial x)(t, 1, y) = 0$. With these conditions, the solution for $\theta(t, x, y)$ is uniquely determined by four inputs into the equation: Pe , H/L , u , and v . u and v are uniquely determined by Re and H/L by solving the momentum equation (in streamfunction-vorticity formulation)

for fully-developed flow. As a consequence, the complete list of scaled inputs into the equation is Pe , Re , and H/L for a rectangular droplet in a long channel.

In the usual way, we nondimensionalize the heat transfer coefficient, h , to define the Nusselt number, Nu , as

$$\text{Nu} = \frac{hH}{k}, \quad (20)$$

where k is the fluid's thermal conductivity. $\text{Nu}(x)$ is calculated from the solution for θ by

$$\text{Nu} = \frac{\frac{\partial \theta}{\partial y}(x, 0)}{\theta_{\text{avg}}(x)} \quad (21)$$

where

$$\theta_{\text{avg}}(x) = \int_0^1 \theta(x, y) \frac{u}{U} dy. \quad (22)$$

Plots of Nusselt number will be made with Nu on the y -axis and $t/\text{Pe} = (xL/H)/\text{Pe}$, the scale distance from the entrance into the heated region, on the x -axis; different values of H/L , Re and Pe will be specified for each individual graph. Note that t/Pe is equivalent to the usual scaled coordinate used for plotting Nusselt number solutions in most heat transfer texts [41].

B. Parameterization

The question may arise: why are there so many more variables to consider when plotting DHT results than in presenting results for continuous Graetz flow? First, the Peclet number in DHT is not assumed to be much greater than unity, and thus enters into the calculations independent of other variables, as it does for generalized continuous thermal entry flow [41]. The effect of L/H on the flow field is also not present in a continuous channel, adding yet another new physical variable to the problem. As a consequence, these three additional variables must be specified when presenting plots of Nusselt number vs. position for digitized flows. When curved interfaces and heat devices of finite length are considered, the effect of meniscus curvature must be included both in determining the velocity field and temperature field, and the effect of device length must be included in determining the temperature profile.

C. Limiting Solutions

To reproduce the well-known result of continuous, hydrodynamically fully developed, steady Graetz flow in a channel, we let $v \rightarrow 0$, $H/L \rightarrow 0$ and $\partial/\partial t \rightarrow 0$ in (19), and start the heated region at $x = 0$. The equation then reduces to

$$u \frac{\partial \theta}{\partial x} = \frac{1}{\text{Pe}} \frac{\partial^2 \theta}{\partial y^2} \quad (23)$$

where u has the usual Poiseuille velocity profile,

$$\frac{u}{U} = 6(y - y^2). \quad (24)$$

(Recall that y has been nondimensionalized by H , and runs from 0 at the channel bottom to 1 at its top.) Please note that this is the only time we consider the flow to be steady; in all other sections of this paper, we find the temporally developed flow as a function of location within a translating droplet.

A second solution is found for a droplet in which only axial diffusion is considered, ignoring all internal convection. This limit is approached both for a very long droplet ($H/L \rightarrow \infty$) or for a droplet with very low Peclet number (fast diffusion). In the latter situation, rapid thermal diffusion causes the velocity terms to be negligible, and the problem becomes completely independent of the axial coordinate within the droplet. The full equation then reduces to

$$\frac{\partial \theta}{\partial t} = \frac{1}{\text{Pe}} \frac{\partial^2 \theta}{\partial y^2} \quad (25)$$

which has the same form as (23) except for the absence of the parabolic velocity profile.

A plot comparing these two solutions is given in Fig. 8. For these two limiting cases, Nu is a function of t/Pe only; for all other cases, it will be necessary to include all the parameters of Section IV-B. Note that the solutions vary considerably for small values of t/Pe ; this is because for the idealized droplet, the heated boundary condition is applied immediately and uniformly to the droplet's length, eliminating the effect of axial convection from the problem and significantly increasing the Nusselt number. While this is an idealized limit, it serves to demonstrate the increase in heat transfer gained by the limiting of axial convection in a digitized flow.

This behavior is similar to the effect of decreasing the Peclet number when axial diffusion is included in general thermal entry flow; see [41, Fig. 3.15] for reference. In each case, the effect of axial convection is limited and the Nusselt number increases near the channel entry, while asymptoting to a similar value. While (25) may at first seem to be an oversimplified idealization, it nevertheless closely matches solutions to the full (19) when $\text{Pe} \ll 1$. This limit is achievable when highly conductive liquid metals or alloys are used as a DHT fluid. See Fig. 9, which was calculated using the physical properties of mercury.

D. Periodic Mixing

For droplets with low values of the Peclet number, radial and axial diffusion will dominate other processes in the configuration considered here. In this case, internal mixing caused by circular convection inside each fluid slug has a minimal effect on the developing temperature of the droplet. For droplets with higher values of Pe, however, convection becomes an increasingly important, and even dominant, physical mechanism for developing the internal temperature profile. For droplets with $\text{Pe} \gg 1$, this imposes a periodic fluctuation on results for the average Nusselt number of a translating fluid slug. This is caused by the internal caterpillar-like circulation periodically bringing cooler fluid into contact with the heated channel walls, thus increasing the temperature gradient at the droplet boundary and increasing heat flux into the droplet. The rough period for this circulation is simply $2(L + .5H)/U$, or the rough distance traveled by a fluid element in one circulation divided by the droplet velocity.

As seen in Fig. 10(a) and (b), this convection results in greater internal mixing and drastically increased overall flux into the droplet when Pe is large. As the droplet approaches the wall temperature, and hence its asymptotic value of Nu, the effect of the periodicity is damped out and Nu approaches a constant,

as with continuous thermal entry flow. The Nusselt number, which characterizes the degree to which convection enhances heat transfer, is greatly increased by the circulation, however. The more narrow the droplet, the greater the effect of circulation and the higher the asymptotic value of Nu. In addition, the greater the Peclet number the greater the relative effect of circulation, and, again, the greater the asymptotic Nusselt number.

Our group has already constructed a program to incorporate curved droplet interfaces into the fluid dynamics. Inclusion of the curved boundaries has the effect of carrying unheated fluid forward into the channel, as well as spreading out distance between droplets, resulting in intermittent patches of no fluid contact with the channel wall. In addition, it also has an effect on the fluid dynamics of the internal circulation of the droplet itself.

V. CONCLUSION

Increases in packaging density and performance have brought thermal issues to the forefront of design for compact electrical systems. This paper proposed DHT of liquids, including liquid alloys and metals, for active thermal management of high power micro systems. Electrowetting on dielectric is a low power, cost-effective and simple approach for active control of fluids used in DHT. The velocity of droplets actuated by this method was presented, as well as solutions for their internal droplet flow fields. Numerical investigations of the coupled mass, momentum and energy equations demonstrated that the nondimensionalized heat transfer coefficients of discretized flows can be several times higher than corresponding continuous flows. A periodic fluctuation in Nusselt number was discovered and characterized, and dimensional analysis was performed to parameterize the DHT method in terms of system variables. This analysis clearly indicated that DHT is a viable new paradigm for thermal management of both steady-state heating and transient power spikes present in a compact electronic device.

REFERENCES

- [1] S. Garmella, Y. Joshi, A. Bar-Cohen, A. Mahajong, K. Toh, V. Carey, M. Baellmans, J. Lohan, B. Sammakia, and F. Andros, "Thermal challenges in next generation electronic systems—Summary of panel presentations and discussions," *IEEE Trans. Compon. Packag. Technol.*, vol. 25, no. 4, pp. 569–575, Dec. 2002.
- [2] V. Singhal, S. Garimella, and A. Raman, "Microchannel pumping technologies for microchannel cooling systems," *Appl. Mech. Rev.*, vol. 57, no. 3, pp. 191–221, 2004.
- [3] "Thermal Management Technology Roadmap of the National Electronics Manufacturing Initiative (NEMI)," Office of the Secretary of Defense, 2002.
- [4] D. Tuckerman and R. Pease, "High performance heat sinking for VLSI," *IEEE Electron Device Lett.*, vol. EDL-2, no. 5, pp. 126–129, May 1981.
- [5] S. Garimella and C. Sobhan, "Transport in microchannels—a critical review," *Annu. Rev. Heat Transf.*, vol. 13, pp. 1–50, 2003.
- [6] A. Miner and U. Ghosal, "Cooling of high-power-density microdevices using liquid metal coolants," *Appl. Phys. Lett.*, vol. 85, no. 3, pp. 506–508, 2004.
- [7] D. Kercher, J.-B. Lee, O. Brand, M. Allen, and A. Glezer, "Microjet cooling devices for thermal management of electronics," *Proceedings of IEEE Trans. Compon. Packag. Technol.*, vol. 26, no. 2, pp. 359–366, Jun. 2003.
- [8] A. Shakouri and J. Bowers, "Heterostructure integrated thermionic coolers," *Appl. Phys. Lett.*, vol. 71, no. 9, pp. 1234–1236, 1997.
- [9] A. Shakouri, C. Labounty, P. Abraham, J. Piprek, and J. Bowers, "Enhanced thermionic emission cooling in high barrier superlattice heterostructures," in *Proc. Mater. Res. Soc. Symp.*, Dec. 1998, vol. 545, pp. 449–458.

- [10] J. Fluerial, A. Borshchevsky, M. Ryan, W. Phillips, E. Kolawa, T. Kacisch, and R. Ewell, "Thermoelectric microcoolers for thermal management applications," in *Proc. IEEE Conf. Thermoelect.*, 1997, pp. 641–645.
- [11] M. Pollack, R. Fair, and A. Shenderov, "Electrowetting-based actuation of liquid droplets for microfluidic applications," *Appl. Phys. Lett.*, vol. 77, no. 11, pp. 1725–1726, 2000.
- [12] M. Pollack, A. Shenderov, and R. Fair, "Electrowetting-based actuation of droplets for integrated microfluidics," *Lab Chip*, vol. 2, no. 2, pp. 96–101, 2002.
- [13] K. Wang and T. Jones, "Electrowetting dynamics of microfluidic actuation," *Langmuir*, vol. 21, pp. 4211–4217, 2005.
- [14] J. Lee and C. Kim, "Liquid micromotor driven by continuous electrowetting," in *Proc. IEEE Micro Electro Mech. Syst. Workshop*, Heidelberg, Germany, Jan. 1998, pp. 538–543.
- [15] S. Cho, H. Moon, and C. Kim, "Creating, transporting, cutting, and merging liquid droplets by electrowetting-based actuation for digital microfluidic circuits," *J. MEMS*, vol. 12, no. 1, pp. 70–80, 2003.
- [16] J. Lee, H. Moon, J. Fowler, T. Schoellhammer, and C. Kim, "Electrowetting and electrowetting-on-dielectric for microscale liquid handling," *Sens. Act., Phys. A*, vol. 95, pp. 259–268, 2002.
- [17] A. Dolatabadi, K. Mohseni, and A. Arzpeyma, "Behaviour of a moving droplet under electrowetting actuation: Numerical simulation," *Can. J. Chem. Eng.*, vol. 84, no. 1, pp. 17–21, 2006.
- [18] K. Mohseni and A. Dolatabadi, "An electrowetting microvalve: Numerical simulation," *Annal. New York Acad. Sci.*, vol. 1077, no. 1, pp. 415–425, 2006.
- [19] F. Mugele and J. C. Baret, "Electrowetting: From basics to applications," *J. Phys.: Condensed Matter*, vol. 17, no. 28, pp. R705–R774, 2005.
- [20] P. Paik, V. Pamula, M. Pollack, and R. Fair, "Electrowetting-based droplet mixers for microfluidic systems," *Lab Chip*, vol. 3, no. 1, pp. 28–33, 2003.
- [21] V. Srinivasan, V. Pamula, M. Pollack, and R. B. Fair, "Clinical diagnostics on human whole blood, plasma, serum, urine, saliva, sweat, and tears on a digital microfluidic platform," in *Proc. μ TAS*, 2003, pp. 1287–1290.
- [22] K. Mohseni, E. Baird, and H. Zhao, "Digitized heat transfer for thermal management of compact microsystems," in *Proc. ASME Int. Mech. Eng. Congress R & D Expo*, Orlando, FL, Nov. 5–11, 2005, p. 79372.
- [23] K. Mohseni, "Effective cooling of integrated circuits using liquid alloy electrowetting," in *Proc. Semicond. Therm. Meas., Model., Manag. Symp. (SEMI-Therm)*, San Jose, CA, Mar. 15–17, 2005, pp. 20–25.
- [24] K. Mohseni and E. Baird, "Digitized heat transfer using electrowetting on dielectric," *Nanoscale Microscale Thermophys. Eng.*, vol. 11, no. 1 & 2, pp. 99–108, 2007.
- [25] K. Mohseni and E. S. Baird, "Digitized heat transfer: Thermal management of compact micro systems using electrostatic droplet actuation," in *Proc. 39th AIAA Thermophys. Conf.*, Miami, FL, Jun. 25–28, 2007.
- [26] V. Pamula and K. Chakrabarty, "Cooling of integrated circuits using droplet-based microfluidics," in *Proc. ACM Great Lakes Symp. VLSI*, 2003, pp. 84–87.
- [27] F. Saeki, J. Baum, H. Moon, J. Yoon, and C. Kim, "Electrowetting on dielectrics: Reducing voltage requirements for microfluidics," *Polym. Mater. Sci. Engr.*, vol. 222, no. 85, pp. 12–13, 2001.
- [28] H. Moon, S. Cho, R. Garrell, and C. Kim, "Low voltage electrowetting-on-dielectric," *J. Appl. Phys.*, vol. 92, no. 7, pp. 4080–4087, 2002.
- [29] E. Baird, P. Young, and K. Mohseni, "Electrostatic force calculation for an EWOD-actuated droplet," *Microfluid Nanofluid* Jan. 2007 [Online]. Available: <http://www.springerlink.com/content/28855500160011k0/>
- [30] K. Mohseni and E. Baird, "A unified velocity model for digital microfluidics," *Nanoscale Microscale Thermophys. Eng.*, vol. 11, no. 1 & 2, pp. 109–120, 2007.
- [31] C. Cooney, C.-Y. Chen, A. Nadim, and J. Sterling, "Electrowetting droplet microfluidics on a single planar surface," *Microfluid Nanofluid* Mar. 2006 [Online]. Available: <http://www.springerlink.com/content/q888262714470714/>
- [32] A. Darhuber, J. Valentino, S. Troian, and S. Wagner, "Microfluidic actuation by modulation of surface stresses," *Appl. Phys. Lett.*, vol. 82, p. 657, 2003.
- [33] J. Chen, S. Troian, A. Darhuber, and S. Wagner, "Effect of contact angle hysteresis on thermocapillary droplet actuation," *J. Appl. Phys.*, vol. 97, no. 1, pp. 014906–014909, Jan. 2005.
- [34] S. Oleg and N. Alexander, "Thermocapillary flows under an inclined temperature gradient," *J. Fluid Mech.*, vol. 504, pp. 99–132, 2004.
- [35] P. Gascoyne, J. Vykoukal, J. Schwartz, T. Anderson, D. Vykoukal, K. Current, C. McConaghy, F. Becker, and C. Andrews, "Dielectrophoresis-based programmable fluidic processors," *Lab Chip*, vol. 4, no. 4, pp. 299–309, 2004.
- [36] T. Jones, "On the relationship of dielectrophoresis and electrowetting," *Langmuir*, vol. 18, pp. 4437–4443, 2002.
- [37] T. Jones and K. Wang, "Frequency-dependent electromechanics of aqueous liquids: Electrowetting and dielectrophoresis," *Langmuir*, vol. 20, pp. 2813–2818, 2004.
- [38] G. Beni, S. Hackwood, and J. Jackel, "Continuous electrowetting effect," *Appl. Phys. Lett.*, vol. 40, no. 10, pp. 912–914, 1982.
- [39] J. Lee and C. Kim, "Surface tension driven microactuation based on continuous electrowetting," *J. MEMS*, vol. 9, no. 2, pp. 220–225, 2000.
- [40] E. Baird and K. Mohseni, "Surface tension actuation of droplets in microchannels," in *Proc. ASME Int. Mech. Eng. Congress R & D Expo*, Orlando, FL, Nov. 5–11, 2005, p. 79371.
- [41] A. Bejan, *Convection Heat Transfer*, 2nd ed. New York: Wiley-Interscience, 1994.
- [42] K. Yun, I. Cho, J. Bu, C. Kim, and E. Yoon, "A surface tension driven micropump for low-voltage and low-power operations," *IEEE J. MEMS*, vol. 11, no. 5, pp. 454–461, Oct. 2002.
- [43] R. Remsburg, Ed., *Advanced Thermal Design of Electronic Equipment*. New York: Chapman & Hall, 1998.
- [44] I. Mudawar, "Assessment of high-heat-flux thermal management schemes," in *Proc. IEEE Inter Soc. Conf. Thermal Phenom.*, Jun. 2000, vol. 24, no. 2, pp. 122–141.
- [45] R. Chu, R. Simons, M. Ellsworth, R. Schmidt, and V. Cozzolino, "Review of cooling technologies for computer products," *IEEE Trans. Device Mater. Reliab.*, vol. 4, no. 4, pp. 568–585, Dec. 2004.
- [46] C. Sobhan and S. Garimella, "A comparative analysis of studies on heat transfer and fluid flow in microchannels," *Microscale Thermophys. Eng.*, vol. 5, pp. 293–311, 2001.



Eric Baird received the B.S. degree in physics from Brigham Young University, Provo, UT, in 2002, and the M.S. degree in physics and the M.S. degree in aerospace engineering sciences from the University of Colorado at Boulder, in 2004 and 2006, respectively, where he is currently pursuing the Ph.D. degree in aerospace engineering sciences.

His research includes actuation methods for digital microfluidics and their application to micro scale thermal management.



Kamran Mohseni (M'00) received the B.S. degree from the University of Science and Technology, Tehran, Iran, the M.S. degree in aeronautics from the Imperial College of Science, Technology, and Medicine, London, U.K., and the Ph.D. degree in mechanical engineering from the California Institute of Technology, Pasadena, in 2000.

He is an Associate Professor in the Aerospace Engineering Sciences Department, University of Colorado at Boulder. He joined the University of Colorado in 2001 after a year as a Postdoctoral Fellow in

Control and Dynamical Systems at the California Institute of Technology (Caltech), Pasadena. His research is in microscale transport, vortex dynamics, and biomimetic and fluidic locomotion.

Dr. Mohseni is a member of ASME, APS, SIAM, and AIAA.